Available online at www.sciencedirect.com
ScienceDirect
Trans. Nonferrous Met. Soc. China 24(2014) 1458−1466
Transactions of Nonferrous Metals Society of China
www.tnmsc.cn

Compositional optimization of glass forming alloys based on critical dimension by using artificial neural network

An-hui CAI[1,2], Xiang XIONG[2], Yong LIU[2], Wei-ke AN[1], Guo-jun ZHOU[1], Yun LUO[1], Tie-lin LI[1], Xiao-song LI[1], Xiang-fu TAN[1]

1. College of Mechanical Engineering, Hunan Institute of Science and Technology, Yueyang 414000, China;
2. State Key Laboratory of Powder Metallurgy, Central South University, Changsha 410083, China

Received 25 June 2013; accepted 30 October 2013

Abstract: An artificial neural network (ANN) model was developed for simulating and predicting critical dimension d_c of glass forming alloys. A group of Zr−Al−Ni−Cu and Cu−Zr−Ti−Ni bulk metallic glasses were designed based on the d_c and their d_c values were predicted by the ANN model. Zr−Al−Ni−Cu and Cu−Zr−Ti−Ni bulk metallic glasses were prepared by injecting into copper mold. The amorphous structures and the determination of the d_c of as-cast alloys were ascertained using X-ray diffraction. The results show that the predicted d_c values of glass forming alloys are in agreement with the corresponding experimental values. Thus the developed ANN model is reliable and adequate for designing the composition and predicting the d_c of glass forming alloy.
Key words: critical dimension; glass forming alloy; artificial neural network; metallic glasses

1 Introduction

Metallic glasses have drawn a lot of interests because of their superior physical, mechanical and chemical properties compared with the corresponding crystalline counterparts [1,2]. In particular, the development of bulk metallic glasses (BMGs) widens their applications and extensively triggers the investigation of glass forming ability (GFA) of alloys.

There are many methods for estimating the GFA of glass forming alloys. One includes empirical rule proposed by INOUE and ZHANG [3] and the electron concentration rule proposed by CHEN et al [4]. These rules can not quantitatively estimate the GFA of the alloys and even there are opposite cases [5]. The second method is the characterization parameters, such as K_{gl} [6], ΔT_x [7], T_{rg} [8,9], γ [7, 9], γ^* [10] and v [11]. These parameters can be obtained after the amorphous alloy has been prepared and/or even there are opposite cases [12]. The third method is the mathematical and/or physical equation [9,13−16]. For example, INOUE et al [15] provided an equation for the estimation of critical cooling rate R_c. LU and LIU [9,16] proposed some empirical relationships for the prediction of the R_c. However, the equation includes some parameters which are difficult to obtain and/or their reliability depends on the number of the data. CAI et al [17,18] tried to relate the R_c with the physical and/or chemical parameters. Although better results were obtained and these parameters were also easily calculated, these relationships can not characterize in the commonality. Finally, researchers proposed some models from the thermal, topological and physical points of view. For example, the composition located at deep eutectic point was designed by thermodynamics [19]. It is clear that its result would deviate from the practical case because the formation of the metallic glass is a non-equilibrium solidification procedure. From the topological structure, it was found that the atomic size ratio [20], the average electronegativity difference [21], and the local packing efficiency [22] were strongly related with the GFA of alloys. However, these parameters are difficult to be calculated for the multi-component alloy. PANG et al [23] have recently designed the composition of Ni−Hf amorphous alloys based on the cluster whose type and magnitude are difficult to be defined. GUO and LIU [24], and CAI et al [25] have recently estimated the R_c for the

Foundation item: Project (50874045) supported by the National Natural Science Foundation of China
Corresponding author: An-hui CAI; Tel: +86-730-8648848; E-mail: cah1970@sohu.com
DOI: 10.1016/S1003-6326(14)63213-1

formation of amorphous alloys from the d_c from the thermodynamic point of view. However, the thermodynamic model contains many parameters which are difficult to be measured and depend on the temperature. Among above mentioned parameters, the d_c can be directly used to evaluate the GFA of glass forming alloys. However, the d_c of the glass forming alloy can be obtained through a large number of the experiments and depends on the experimental condition. Can it be quickly and reliably estimated ahead of the experiments?

It is well known that the d_c is influenced by physical and chemical factors. The relationships between the d_c and these factors are very complex, resulting in the difficult description of the relationships by a mathematical and/or physical model. Artificial neural network (ANN) technique is thought to be a reliable method for the resolution of the complex system and has been effectively used for the composition design, technology optimization, and performance prediction [26−33] due to its perfect performance, such as self-organization, self-adaption, strong learning and anti-interference capacity. Moreover, the ANN technique has been used to predict parameters for the metallic glasses and reliable results are obtained. For example, KEONG et al [34] established an ANN model for reliably predicting the crystallization temperatures of the Ni−P based metallic glasses. CAI et al [35−37] established ANN models for predicting T_{rg}, ΔT_x and R_c of glass forming alloy, respectively. But there are no reports for the prediction of the d_c of glass forming alloy by ANN technique.

In the present work, a computer model based on radial basis function artificial neural network (RBFANN) is designed for prediction and simulation of the d_c of metallic glass. In addition, a group of Zr−Al−Ni−Cu bulk metallic glasses are designed and their d_c values are predicted by the RBFANN model. It is found that the predicted d_c values are in good agreement with the corresponding experimental values.

2 Experimental

Zr−Al−Cu−Ni and Cu−Zr−Ti−Ni shown in Tables 1 and 2 alloys with nominal compositions (mole fraction, %) were pre-alloyed more than five times by arc melting pure metal elements in a Ti-gettered argon atmosphere. These master ingots then were surface-polished, followed by induction-melting inside quartz tubes in argon atmosphere, then injected into copper mold to obtain d1−10 mm conical samples. The amorphous structures and the determination of the d_c of as-cast alloys were ascertained using X-ray diffraction (XRD) with a XD-3A diffractometer with Cu K_α.

Table 1 Predicted and tested d_c values for Zr−Al−Ni−Cu bulk metallic glasses developed in this work

Bulk metallic glass	d_c/mm		Error/%
	Tested	Predicted	
$Zr_{54}Al_{13}Cu_{18}Ni_{15}$	6.5	6.6	1.5
$Zr_{60.5}Al_{12.1}Cu_{10.95}Ni_{16.45}$	7.5	8.0	6.7
$Zr_{61.5}Al_{10.7}Cu_{13.65}Ni_{14.15}$	5.5	5.8	5.5
$Zr_{62}Al_{10}Cu_{15}Ni_{13}$	5.0	5.2	4.0
$Zr_{62.5}Al_{12.1}Cu_{7.95}Ni_{17.45}$	7.5	8.1	8.0
$Zr_{63.5}Al_{10.7}Cu_{10.7}Ni_{15.1}$	6.0	6.5	8.3
$Zr_{64}Al_{10.1}Cu_{11.7}Ni_{14.2}$	5.0	5.2	4.0
$Zr_{65}Al_{8.7}Cu_{14.4}Ni_{11.9}$	4.0	4.5	12.5

Table 2 Predicted and tested d_c values for Cu−Zr−Ti−Ni bulk metallic glasses developed in this work

Bulk metallic glass	d_c/mm		Error/%
	Tested	Predicted	
$Cu_{50}Zr_{40}Ti_{10}$	2.0	2.3	15.0
$Cu_{50}Zr_{40}Ti_{9.5}Ni_{0.5}$	3.0	3.2	6.7
$Cu_{50}Zr_{40}Ti_{9}Ni_{1}$	4.0	3.8	5.0
$Cu_{50}Zr_{40}Ti_{8}Ni_{2}$	5.0	5.2	4.0
$Cu_{50}Zr_{40}Ti_{7}Ni_{3}$	3.0	2.8	6.7
$Cu_{50}Zr_{40}Ti_{6}Ni_{4}$	2.0	1.8	10

3 ANN model

Back-propagation artificial neural network (BPANN) and radial basis function artificial neural network RBFANN are thought to be general methods for simulation and prediction modeling. The BPANN has stronger generalization capacity, but it has some shortcomings. It is difficult to determine learning rate, initial weight, objective error, and the numbers of hidden layers and of neurons in hidden layer. Moreover, it would result in the decrease of convergent rate and even be trapped in a local minimum if these parameters can not be suitably and coordinately selected. Nevertheless, the RBFANN has some merits, such as only one adjusted parameter, rapid training procedure and zero error [26−29,35−37]. In addition, the RBFANN is advantageous of the BPANN for better approximating and sorting capacity, and quick learning rate. The base functions among the nodes of the hidden layers for the RBFANN characterize in locality, indicating that the RBFANN is suitable for solving the complex, nonlinear, and local problems. Thus, MATLAB 7.0 package (Neural Network Toolbox from The Math Works Inc.) was used to create the RBFANN model in the present work. The modeling procedures are as follows. Firstly, the data is collected, analyzed and pre-processed. Then the pre-processed data are divided into two kinds of data,

i.e., one for training and the other for testing. The third step is to train the neural network. Lastly, the trained neural network is tested.

Sixteen parameters strongly influencing the d_c are selected for the inputs of RBFANN model. These parameters are mixing entropy (S_{mix}), difference in atomic radius ratio (Δd), average atomic radius (d_e), difference in atomic electronegativity ratio (Δe), average atomic electronegativity (e_e), $\Delta d/\Delta e$, d_e/e_e, ionicity index (v), fusion heat (ΔH_m), fusion temperature (T_m), $\Delta H_m/T_m$, specific heat capacity (c_p), thermal conductivity (λ), density (ρ), thermal diffusivity ($\alpha=\lambda/\rho c_p$), and thermal storage coefficient ($b=(\lambda\rho c_p)^{1/2}$). The reasons for the selection and the calculation of these parameters are shown in Refs. [17,18,24,35−37]. In addition, it should be noted that the d_c is used to be the output of RBFANN model.

4 Results and discussion

The RBFANN model for predicting and simulating the d_c consists of 16 inputs and 1 output. These parameters are calculated by weighted average method with the weight of atomic percentage of each element in metallic glasses [17,18]. Then, these input and output parameters are normalized in the region of (0, 1) to improve the training efficiency according to $X=0.1+0.8(x-x_{min})/(x_{max}-x_{min})$ (X is the normalization parameter, x is a parameter value, x_{min} and x_{max} are the minimum and maximum values for a parameter). The detailed training procedure of the RBFANN is shown in Refs. [35−37]. However, it should be noted that the ratio of the data for training and the datum for testing is confined to be 99:100 during the training and testing procedures. A distribution parameter t was chosen to be 46 because there is the largest linear correlation coefficient (r) between the predicted d_c values and the corresponding experimental values. Furthermore, the developed RBFANN model was verified by the data [38−49] in Table 3 in order to examine its efficiency. The relationship between the predicted d_c and the experimental value is shown in Fig. 1. As shown in Table 3, the predicted d_c values deviate from the corresponding experimental values. However, Fig. 1 presents a better linear relationship and the linear correlation coefficient reaches up to 0.9951, indicating better global performance of the RBFANN model.

In addition, a reliable model should be characterized in not only better global performance but also better local performance including the sorting capacity and the sensitivity to alloying elements. Figure 2 presents the relationships between the predicted d_c values and the corresponding experimental values for Zr-based, Fe-based, Mg-based, Ni-based and Cu-based metallic glasses in Table 3.

Table 3 Predicted and tested d_c values of metallic glasses [38−49]

Metallic glass	d_c/mm	
	Predicted	Tested
$Mg_{79.4}Ni_{10.4}Nd_{10.2}$	0.7	0.6
$Mg_{75.8}Ni_{14.6}Nd_{9.6}$	3.1	2.8
$Mg_{74.9}Ni_{10.1}Nd_{15}$	0.3	0.7
$Mg_{69.3}Ni_{15.5}Nd_{15.2}$	1.7	1.0
$Mg_{76.5}Ni_{18.2}Nd_{5.3}$	0.2	0.1
$Mg_{65.3}Ni_{19.9}Nd_{14.8}$	3.0	3.5
$Mg_{89.4}Ni_{5.4}Nd_{5.2}$	0.1	0.1
$Mg_{65}Cu_{25}Gd_{10}$	7.4	8.0
$Mg_{65}Cu_{20}Gd_{10}Ni_5$	4.3	5.0
$Ni_{57}Ti_{18}Zr_{20}Si_5$	1.8	2.0
$Ni_{57}Pd_{25}P_{18}$	10.6	10.0
$Ni_{47}Ti_{23}Zr_{15}Pd_{10}Si_5$	3.2	3.0
$Ni_{42}Ti_{23}Zr_{15}Pd_{15}Si_5$	3.6	3.0
$Ni_{59}Ti_{13}Zr_{14}Sn_3Nb_9Si_2$	2.6	2.0
$Ni_{40}Ti_{16.5}Zr_{28.5}Al_{10}Cu_5$	4.3	5.0
$Ni_{59}Ti_{16}Zr_{15}Sn_3Nb_5Si_2$	2.3	2.0
$Ni_{59}Ti_{16}Zr_{11}Sn_3Nb_9Si_2$	2.3	2.0
$Ni_{59}Ti_{11}Zr_{18}Sn_3Nb_7Si_2$	2.3	2.0
$Ni_{59}Ti_{11}Zr_{17}Sn_3Nb_8Si_2$	2.5	2.0
$Ni_{59}Ti_9Zr_{20}Sn_3Nb_7Si_2$	2.5	2.0
$Zr_{38}Ti_{17}Cu_{12.5}Be_{22.5}Co_{10}$	11.2	12.0
$Zr_{38}Ti_{17}Cu_{10.5}Be_{22.5}Co_{12}$	11.3	12.0
$Zr_{38}Ti_{17}Cu_{7.5}Be_{22.5}Co_{15}$	11.6	12.0
$Zr_{38}Ti_{17}Be_{22.5}Co_{22.5}$	8.5	8.0
$(Zr_{60}Al_{10}Cu_{20}Ni_{10})_{97.64}Ti_{2.36}$	4.6	4.0
$(Zr_{60}Al_{10}Cu_{20}Ni_{10})_{95.32}Ti_{4.68}$	4.6	4.0
$(Zr_{60}Al_{10}Cu_{20}Ni_{10})_{93.04}Ti_{6.96}$	5.4	5.0
$(Zr_{60}Al_{10}Cu_{20}Ni_{10})_{90.8}Ti_{9.2}$	7.7	7.0
$(Zr_{60}Al_{10}Cu_{20}Ni_{10})_{88.6}Ti_{11.4}$	5.9	6.0
$Zr_{58}Ti_4Al_{10}Cu_{20}Ni_8$	4.5	3.0
$Zr_{59}Ti_3Al_{10}Cu_{20}Ni_8$	4.4	3.0
$Zr_{52}Ti_5Al_{10}Cu_{18}Ni_{15}$	5.6	3.0
$Zr_{51.92}Ti_{5.28}Al_{12}Cu_{19.36}Ni_{11.44}$	5.2	5.0
$Zr_{50.56}Ti_{5.14}Al_{14.3}Cu_{18.85}Ni_{11.14}$	5.6	5.0
$Zr_{46.75}Ti_{8.25}Cu_{7.5}Ni_{10}Be_{27.5}$	10.7	10.0
$Zr_{38}Ti_{17}Cu_{12.5}Ni_{10}Be_{22.5}$	11.6	12.0
$Zr_{41}Ti_{14}Cu_{12.5}Be_{22.5}Co_{10}$	11.0	12.0
$Zr_{38}Ti_{17}Cu_{12.5}Ni_5Be_{22.5}Co_5$	11.0	12.0
$Fe_{65.65}P_{11.94}Mo_{3.98}C_{4.97}B_{5.5}Ga_{3.98}Cr_{3.98}$	4.0	4.0
$Fe_{50}Co_{10}Mo_{14}C_{16}B_6Cr_4$	4.4	4.0
$Fe_{76.7}Nb_6B_{17}Y_{0.3}$	0.2	0.3
$Fe_{76.4}Nb_6B_{17}Y_{0.6}$	0.4	0.4
$Fe_{76.1}Nb_6B_{17}Y_{0.9}$	0.3	0.3
$Fe_{75.5}Nb_6B_{17}Y_{1.5}$	0.6	0. 5
$Fe_{75}Nb_6B_{17}Y_2$	1.0	0.6
$Fe_{74.5}Nb_6B_{17}Y_{2.5}$	1.5	0.7
$Fe_{74}Nb_6B_{17}Y_3$	2.0	0.8

to be continued

Continued

Metallic glass	d_c/mm	
	Predicted	Tested
$Cu_{65}Ti_5Zr_{35}$	3.8	3.0
$Cu_{65}Ti_{7.5}Zr_{32.5}$	5.3	5.0
$Cu_{65}Ti_{10}Zr_{30}$	5.2	5.0
$Cu_{65}Ti_{12.5}Zr_{27.5}$	4.9	5.0
$Cu_{65}Ti_{15}Zr_{25}$	3.5	4.0
$Cu_{65}Ti_{17.5}Zr_{22.5}$	2.8	3.0
$Cu_{65}Ti_{20}Zr_{20}$	2.8	3.0
$Cu_{65}Ti_{22.5}Zr_{17.5}$	2.6	3.0
$Cu_{65}Ti_{25}Zr_{15}$	2.7	3.0
$Cu_{65}Ti_{27.5}Zr_{12.5}$	2.8	3.0

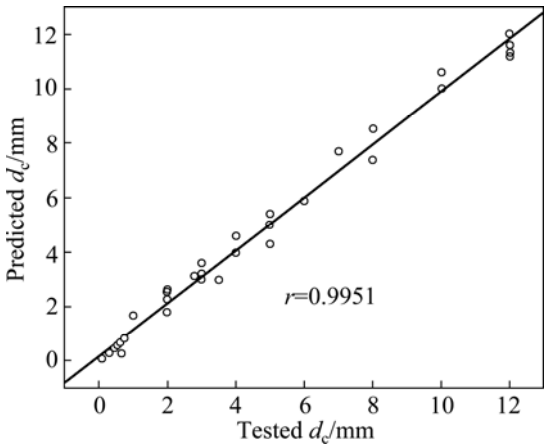

Fig. 1 Relationship between predicted and corresponding tested d_c values of metallic glasses in Table 3

It is observed from Fig. 2 that the linear correlation coefficients are 0.9837 for Zr-based metallic glasses, 0.9610 for Fe-based metallic glasses, 0.9887 for Mg-based metallic glasses, 0.9868 for Ni-based metallic glasses, and 0.9344 for Cu-based metallic glasses, respectively. It indicates that the established RBFANN model characterizes in better sorting performance. Of course, there is a difference among the linear correlation coefficients for different alloy systems. It would be due to the different magnitude of samples in the RBFANN model and/or the accuracy of the experimental d_c values for different alloy systems.

The sensitivity to large and minor change of the alloying elements is also investigated and presented in Fig. 3. It is clearly seen from Fig. 3 that although the predicted d_c values deviate from the corresponding tested values, the change tendency of the predicted d_c values to the alloying elements is in good agreement with that of the tested values except for $Cu_{60}Ti_{40-x}Zr_x$ metallic glasses of 12.5%≤x≤22.5% and 27.5%≤x≤32.5% (Fig. 3(a)) and $Zr_{38}Ti_{17}Cu_{22.5-x}Be_{22.5}Co_x$ metallic glasses of 10%≤x≤15%

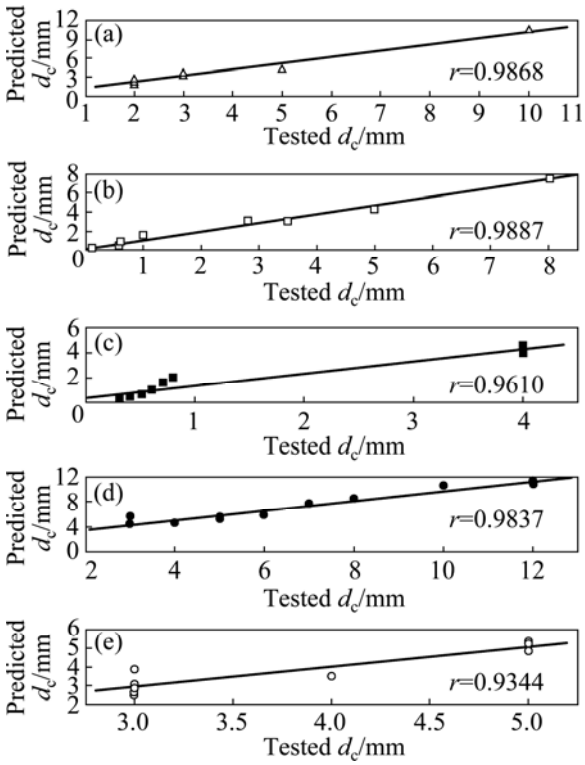

Fig. 2 Relationships between predicted d_c and corresponding d_c value for Ni-based (a), Mg-based (b), Fe-based (c), Zr-based (d), and Cu-based (e) metallic glasses, respectively

(Fig. 3(b)). Thus, the established RBFANN model is sensitive to the compositional change of the metallic glass.

Furthermore, the d_c values of other 218 metallic glasses were predicted whose tested d_c values are uncertain, as shown in Fig. 4. Although the values between the predicted d_c values and the corresponding tested values are different from each other (not shown here), the linear correlation coefficient is up to 0.9220 (Fig. 4). It indicates better change tendency between the predicted d_c values and the tested d_c values.

The d_c values of Al-based metallic glasses [50−54] with worse GFA were predicted by the established RBFANN model, as shown in Table 4. It is obviously from Table 4 that the predicted and tested d_c values of the Al-based metallic glasses are in better agreement with each other. The linear correlation coefficient is up to 0.9347 (Fig. 5(a)), indicating that the predicted and tested d_c values of the Al-based metallic glasses are in better agreement with each other in the change tendency. Interestingly, it is found from Fig. 5(b) that the change tendency for the predicted d_c of $Al_{85}Ni_5Y_{8-x}Co_2Fe_x$ (1≤x≤5) to Fe content is in better agreement with that for the corresponding tested ones. Thus, the established RBFANN model is reliable and adequate.

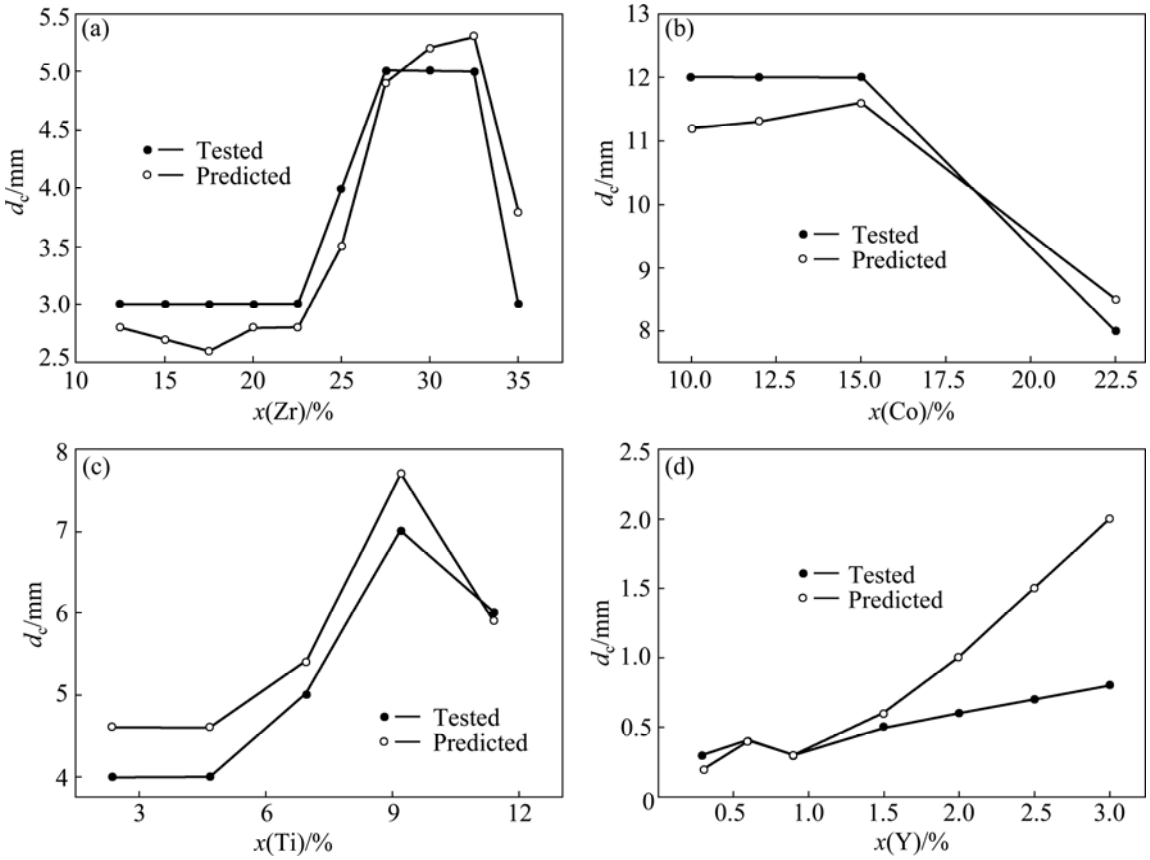

Fig. 3 Change of predicted and tested d_c values of $Cu_{60}Ti_{40-x}Zr_x$ metallic glasses on Zr (a), $Zr_{38}Ti_{17}Cu_{22.5-x}Be_{22.5}Co_x$ metallic glasses on Co (b), $(Zr_{60}Al_{10}Cu_{20}Ni_{10})_{100-x}Ti_x$ metallic glasses on Ti (c), and $Fe_{77-x}Nb_6B_{17}Y_x$ metallic glasses on Y (d)

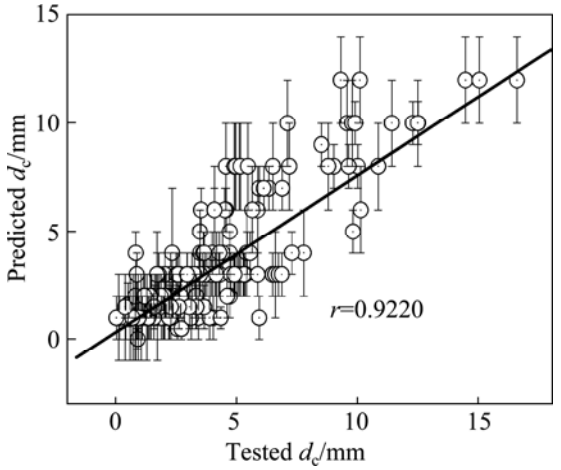

Fig. 4 Relationship between predicted d_c and tested values of some metallic glasses

On the other hand, the compositions of a group of Zr−Al−Ni−Cu metallic glasses [12,55−57] were optimized by the established RBFANN model and their d_c values were carefully defined by XRD results (not shown herein). The tested and predicted d_c values are listed in Table 1. As shown in Table 1, although the error between the tested and the predicted d_c values of

Table 4 Predicted and tested d_c values for Al-based metallic glasses [50−54]

Metallic glass	d_c/mm	
	Tested	Pred.
$Al_{85}Ni_5Y_3Co_2Fe_5$	0.58	0.79
$Al_{85}Ni_5Y_4Co_2Fe_4$	0.48	0.68
$Al_{85}Ni_5Y_5Co_2Fe_3$	0.38	0.46
$Al_{85}Ni_5Y_7Co_2Fe_1$	0.15	0.23
$Al_{83}Ni_{7.9}Y_{9.1}$	0.23	0.35
$Al_{82}Ni_{8.4}Y_{9.6}$	0.25	0.21
$Al_{81}Ni_{8.9}Y_{10.1}$	0.28	0.38
$Al_{85}Ni_5Y_4Co_2Nd_4$	0.95	1.43
$Al_{84}Ni_{7.5}Y_{8.5}$	0.20	0.28
$Al_{85}Ni_3Y_8Co_2Cu_2$	0.23	0.16
$Al_{85}Ni_4Y_8Co_2Cu_1$	0.16	0.10
$Al_{85}Ni_8Y_5Co_2$	0.47	0.38
$Al_{79}Ni_{9.8}Y_{11.2}$	0.34	0.27
$Al_{78}Ni_{10.3}Y_{11.7}$	0.37	0.31
$Al_{77}Ni_{10.7}Y_{12.3}$	0.40	0.35
$Al_{75}Ni_{11.7}Y_{13.3}$	0.47	0.41

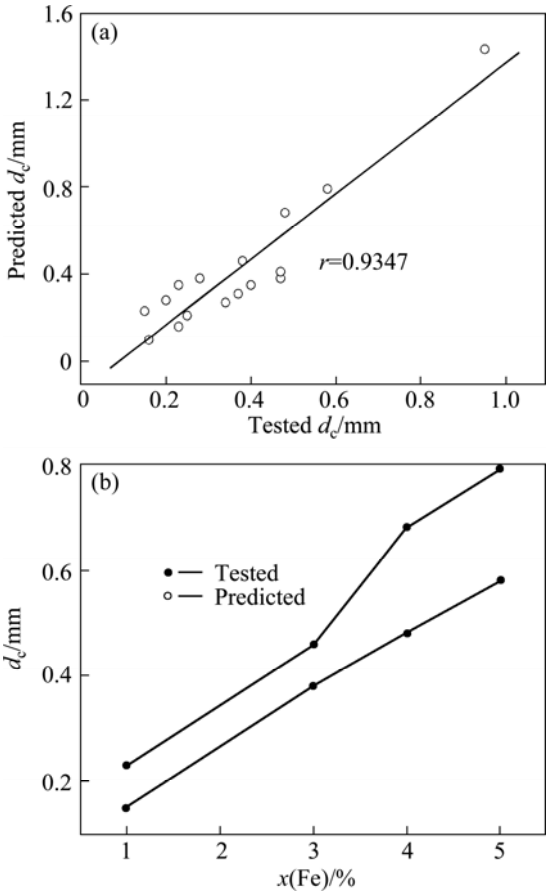

Fig. 5 Relationship between predicted and tested d_c values of $Al_{85}Ni_5Co_2Y_{8-x}Fe_x$ (x=1,3,4,5) metallic glasses listed in Table 4 (a), and change of predicted and tested d_c values for $Al_{85}Ni_5Y_{8-x}Co_2Fe_x$ metallic glasses on Fe (b)

$Zr_{63.5}Al_{10.7}Cu_{10.7}Ni_{15.1}$ metallic glass is up to 12.5%, the errors for other Zr−Al−Ni−Cu metallic glasses do not exceed 10%. It indicates that the predicted d_c of Zr−Al−Ni−Cu metallic glasses accord with the corresponding tested values. In addition, the relationship between the predicted d_c values and the tested values is presented in Fig. 6. It is clearly seen from Fig. 6 that the predicted d_c values of Zr−Al−Ni−Cu metallic glasses are in better agreement with the tested ones because the linear correlation coefficient is up to 0.9911.

In order to further examine the reliability of the RBFANN model, Cu−Zr−Ti−Ni glass forming alloys were also designed by the RBFANN. Their compositions are shown in Table 2. Their amorphous structures were ascertained by XRD and their XRD patterns are presented in Fig. 7. The d_c values of Cu−Zr−Ti−Ni bulk metallic glasses developed in this work can be determined according to Fig. 7 and are listed in Table 2.

As shown in Table 2, although the d_c error of $Cu_{50}Zr_{40}Ti_{10}$ bulk metallic glass is up to 15.0%, the errors of other Cu−Zr−Ti−Ni bulk metallic glasses do not

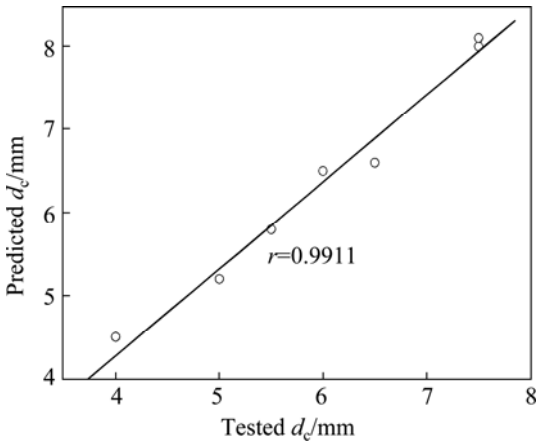

Fig. 6 Relationship between predicted d_c values and tested d_c values of Zr−Al−Ni−Cu bulk metallic glasses developed in this work as shown in Table 1

exceed 10.0%. It indicates that the predicted d_c values of Cu−Zr−Ti−Ni bulk metallic glasses are in good agreement with the corresponding tested values. In addition, the relationship between the predicted d_c values and the tested values is shown in Fig. 8(a). One can clearly observe from Fig. 8(a) that the linear correlation coefficient is up to 0.9801, indicating that the predicted and tested d_c values of Cu−Zr−Ti−Ni bulk metallic glasses agree with each other. Figure 8(b) presents the change of the predicted and tested d_c values of Cu−Zr−Ti−Ni bulk metallic glasses to Ni content. It is clearly observed from Fig. 8(b) that the change tendency of the predicted d_c values is in good agreement with that of the corresponding tested values. It also indicates that the developed RBFANN model is sensitive to the Ni content in Cu−Zr−Ti−Ni glass forming alloys. In a word, the established RBFANN model can be reliably used to design the composition and predict the d_c of glass forming alloy.

5 Conclusions

1) The RBFANN model can identify the type of alloys and elements and is sensitive to large and minor change of alloying elements, indicating its global, local, and sorting performance. The predicted results are in good agreement with the corresponding experimental values, indicating that the RBFANN model developed in this work is reliable and adequate for the prediction and the simulation of the critical dimension of glass forming alloys.

2) The predicted d_c values of Zr−Al−Ni−Cu and Cu−Zr−Ti−Ni bulk metallic glasses developed in this work are in good agreement with the corresponding

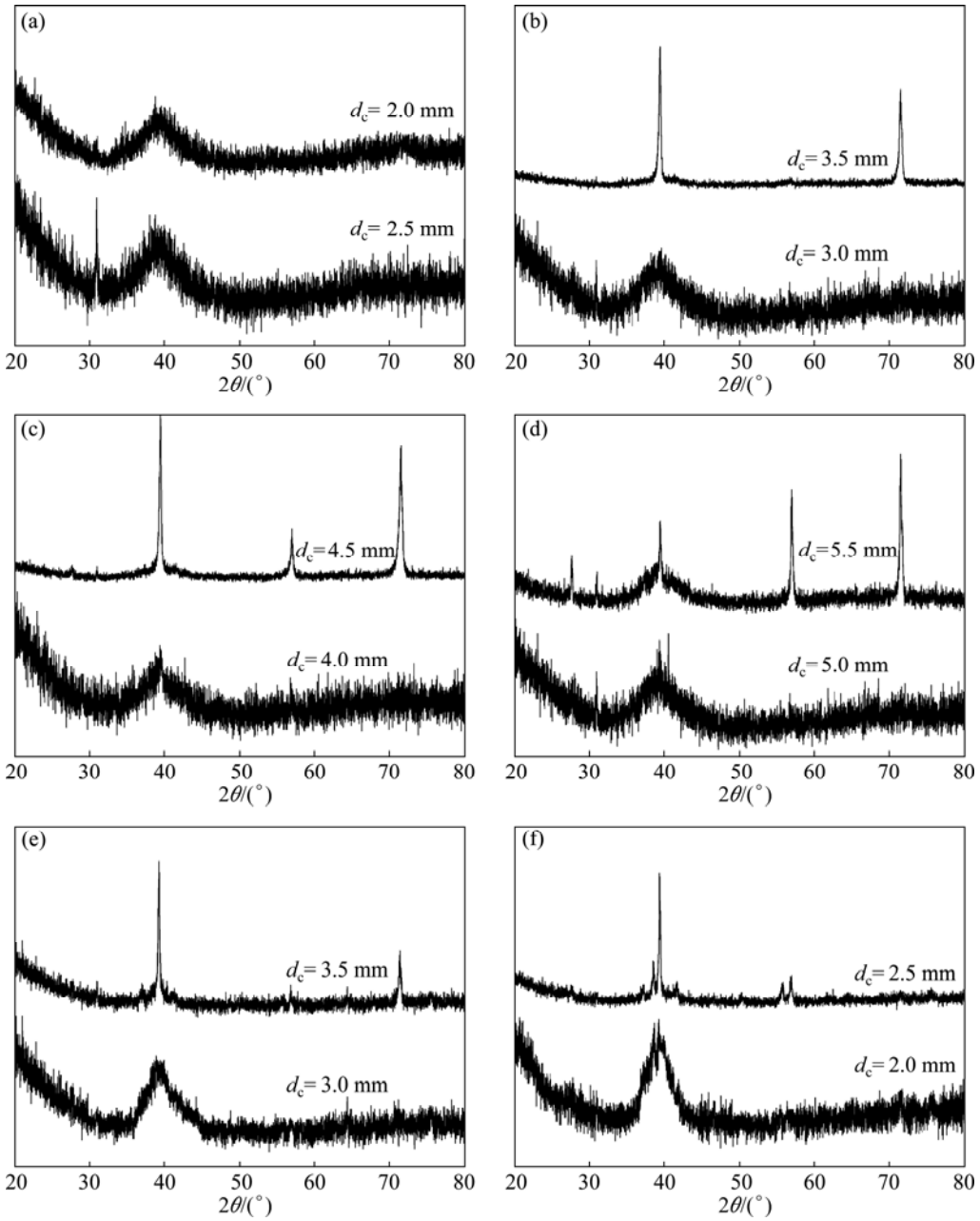

Fig. 7 XRD patterns of $Cu_{50}Zr_{40}Ti_{10-x}Ni_x$ ($0 \le x \le 4\%$): (a) x=0; (b) x=0.5%; (c) x=1%; (d) x=2%; (e) x=3%; (f) x=4%

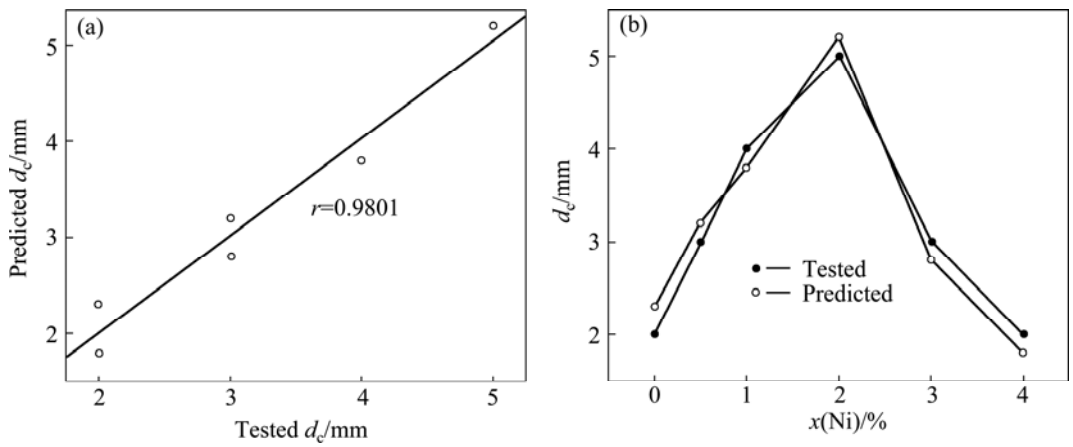

Fig. 8 Relationship between predicted d_c values and tested d_c values (a) and change tendency of predicted and tested d_c values to Ni content (b) for Cu−Zr−Ti−Ni bulk metallic glasses developed by us in Table 2

experimental values. The change tendency of the predicted d_c values is also in good agreement with that of the corresponding tested values. These results indicate that RBFANN model could be reliably used to optimize the compositions and predict the critical dimensions of glass forming alloys.

References

[1] WANG W H, DONG C, SHEK C H. Bulk metallic glasses [J]. Mater Sci Eng R, 2004, 44: 45−89.

[2] WANG W H. Roles of minor additions in formation and properties of bulk metallic glasses [J]. Prog Mater Sci, 2007, 52: 540−596.

[3] INOUE A, ZHANG T. Stabilization of super-cooled liquid and bulk glassy alloys in ferrous and non-ferrous systems [J]. J Non-Cryst Solids, 1999, 250−252: 552−557.

[4] CHEN W, WANG Y, QIANG J, DONG C. Bulk metallic glasses in the Zr−Al−Ni−Cu system [J]. Acta Mater, 2003, 51: 1899−1907.

[5] SCHWARZ R B, HE Y. Formation and properties of bulk amorphous Pd−Ni−P alloys [J]. Mater Sci Forum, 1997, 235: 231−233.

[6] HURBY A. Evaluation of glass-forming tendency by means of DTA [J]. Czech J Phys, 1972, 22: 1187−1193.

[7] LI Y, NG S C, ONG C K, HNG H H, GOH T T. Glass forming ability of bulk glass forming alloys [J]. Scripta Mater, 1997, 36: 783−787.

[8] LU Z P, TAN H, LI Y. The correlation between reduced glass transition temperature and glass forming ability of bulk metallic glasses [J]. Scripta Mater, 2000, 42: 667−673.

[9] LU Z P, LIU C T. A new glass-forming ability criterion for bulk metallic glasses [J]. Acta Mater, 2002, 50: 3501−3512.

[10] XIA L, FANG S S, WANG Q, DONG Y D, LIU C T. Thermodynamic modeling of glass formation in metallic glasses [J]. Appl Phys Lett, 2006, 88: 171905.

[11] WANG W H. The elastic properties, elastic models and elastic perspectives of metallic glasses [J]. Prog Mater Sci, 2012, 57: 487−656.

[12] CAI A H, XIONG X, LIU Y, AN W K, TAN J Y, PAN Y. Design of new Zr−Al−Ni−Cu bulk metallic glasses [J]. J Alloys Compd, 2009, 468: 432−437.

[13] CAI A H, CHEN H, AN W K, TAN J Y, ZHOU Y. Relationship between melting enthalpy ΔH_m and critical cooling rate R_c for bulk metallic glasses [J]. Mater Sci Eng A, 2007, 457: 6−12.

[14] CAI A H, PAN Y, GU J, SUN G X. A new criterion for glass forming ability of bulk metallic glasses [J]. Mater Sci Technol, 2006, 22: 859−863.

[15] INOUE A, ZHANG T, MASUMOTO T. Glass-forming ability of alloys [J]. J Non-Cryst Solids, 1993, 156−158: 473−480.

[16] LU Z P, LIU C T. Glass formation criterion for various glass-forming systems [J]. Phys Rev Lett, 2003, 91: 115505.

[17] CAI A H, SUN G X, PAN Y. Evaluation of the parameters related to glass-forming ability of bulk metallic glasses [J]. Mater Des, 2006, 27: 479−488.

[18] CAI A H, PAN Y, SUN G X. New thermodynamic parameter describing glass forming ability of bulk metallic glasses [J]. Mater Sci Technol, 2005, 21: 1222−1226.

[19] CAO H B, MA D, HSIEH K C, DING L, STRATTON W G, VOYLES P M, PAN Y, CAI M D, DICKINSON J T, CHANG Y A. The correlation between reduced glass transition temperature and glass forming ability of bulk metallic glasses [J]. Acta Mater, 2006, 54: 2975−2982.

[20] EGAMI T, WASEDA Y. Atomic size effect on the formability of metallic glasses [J]. J Non-Cryst Solids, 1984, 64: 113−134.

[21] BOTTA W J, PEREIRA F S, BOLFARINI C, KIMINAMI C S, OLIVEIRA M F. Topological instability and electronegativity effects on the glass-forming ability of metallic alloys [J]. Philosophical Magazine Letters, 2008, 88: 785−791.

[22] MIRACLE D B. Atomic size effect on the formability of metallic glasses [J]. J Non-Cryst Solids, 2004, 342: 89−96.

[23] PANG Chang, JIANG Jian-bing, LUO Ling-jie, GENG Yao-xiang, WANG Ying-min, WANG Qing, DONG Chuang. Ni−Hf metallic glasses and their atomic cluster formulas [J]. Scientia Sinica: Physica, Mechanica & Astronomica, 2012, 42(5): 592−597. (in Chinese)

[24] GUO S, LIU Y. Estimation of critical cooling rates for formation of amorphous alloys from critical sizes [J]. J Non-Cryst Solids, 2012, 358: 2753−2758.

[25] CAI A H, XIONG X, LIU Y, AN W K, ZHOU G J, LUO Y, LI T L, LI X S. Estimation of glass forming ability of Mg-based alloys based on thermodynamics [J]. J Non-Cryst Solids, 2013, 376: 68−75.

[26] AN W K, CAI A H, LUO Y, CHEN H, LIU W X, LI T L, CHEN M. Optimization of composition of as-cast chromium white cast iron based on wear-resistant performance [J]. Mater Des, 2009, 30: 2339−2344.

[27] CAI A H, CHEN H, AN W K, LI X S, ZHOU Y. Optimization of composition and technology for phosphate graphite mold [J]. Mater Des, 2008, 29: 1835−1839.

[28] CAI A H, ZHOU Y, TAN J Y, LUO Y, LI T L, CHEN M, AN W K. Optimization of composition of heat-treated chromium white cast iron casting by phosphate graphite mold [J]. J Alloys Compd, 2008, 466: 273−280.

[29] CAI A H, CHEN H, AN W K, LIU W X, LUO Y, LI T L, CHEN M. Robust optimisation of chemical composition of as cast chromium white cast iron using a green sand mould [J]. Mater Sci Technol, 2008, 24: 302−308.

[30] YANG Xia-wei, ZHU Jing-chuan, NONG Zhi-sheng, HE Dong, LAI Zhong-hong, LIU Ying, LIU Fa-wei. Prediction of mechanical properties of A357 alloy using artificial neural network [J]. Transactions of Nonferrous Metals Society of China, 2013, 23: 788−795.

[31] YANG Xia-wei, ZHU Jing-chuan, HE Dong, LAI Zhong-hong, NONG Zhi-sheng, LIU Yong. Optimum design of flow distribution in quenching tank for heat treatment of A357 aluminum alloy large complicated thin-wall workpieces by CFD simulation and ANN approach [J]. Transactions of Nonferrous Metals Society of China, 2013, 23: 1442−1451.

[32] LIN Yi, ZHENG Zi-qiao, ZHANG Hai-feng, HAN Ye. Effect of heat treatment process on tensile properties of 2A97 Al−Li alloy: Experiment and BP neural network simulation [J]. Transactions of Nonferrous Metals Society of China, 2013, 23: 1728−1736.

[33] SENTHILKUMAR V, BALAJI A, ARULKIRUBAKARAN D. Application of constitutive and neural network models for prediction of high temperature flow behavior of Al/Mg based nanocomposite [J]. Transactions of Nonferrous Metals Society of China, 2013, 23: 1737−1750.

[34] KEONG K G, SHA W, MALINOV S. Artificial neural network modelling of crystallization temperatures of the Ni−P based amorphous alloys [J]. Mater Sci Eng A, 2004, 365: 212−218.

[35] CAI A H, XIONG X, LIU Y, AN W K, TAN J Y. Artificial neural network modeling of reduced glass transition temperature of glass forming alloys [J]. Appl Phys Lett, 2008, 92: 111909.

[36] CAI A H, XIONG X, LIU Y, AN W K, TAN J Y, LUO Y. Artificial neural network modeling for undercooled liquid region of glass

forming alloys [J]. Compt Mater Sci, 2010, 48: 109−114.
[37] CAI A H, LIU Y, AN W K, ZHOU G J, LUO Y, LI T L, LI X S, TAN X F. Prediction of critical cooling rate for glass forming alloys by artificial neural network [J]. Mater Des, 2013, 52: 671−676.
[38] XING Da-wei, SHEN Jun, SUN Jian-fui, WANG Gang, YAN Ming. Glass forming ability of bulk $(Zr_{0.6}Cu_{0.2}Ni_{0.1}Al_{0.1})_{100-x}Ti_x$ amorphous alloys [J]. Journal of Harbin Institute of Technology, 2004, 36(9): 1265−1268. (in Chinese)
[39] WU Xiao-feng, ZHANG Hai-feng, QIU Ke-qiang, YANG Hong-cai, HU Zhuang-qi. Preparation and mechanical properties of Zr-based containing Co bulk metallic glass [J]. Rare Metal Materials and Engineering, 2004, 33(12): 1317−1320. (in Chinese)
[40] ZHANG Tao, MEN Hua, TI Yun-jie. Formation and mechanical properties of Cu−Ti−Zr bulk glassy alloys [J]. Journal of Beijing University of Aeronautics and Astronautics, 2004, 30(10): 925−929.
[41] SONG D S, KIM J H, FLEURY E, KIM W T, KIM D H. Synthesis of ferromagnetic Fe-based bulk glassy alloys in the Fe−Nb−B−Y system [J]. J Alloys Compd, 2005, 389: 159−164.
[42] XU D H, DUAN G, JOHNSON W L, GARLAND C. Formation and properties of new Ni-based amorphous alloys with critical casting thickness up to 5 mm [J]. Acta Mater, 2004, 52: 3493−3497.
[43] WANG L M, LI C F, INOUE A. Formation and mechanical properties of bulk glassy $Ni_{57-x}Ti_{23}Zr_{15}Si_5Pd_x$ alloys [J]. Trans JIM, 2001, 42: 886−889.
[44] LEE J Y, BAE D H, LEE J K, KIM D H. Bulk glass formation in the Ni−Zr−Ti−Nb−Si−Sn alloy system [J]. J Mater Res, 2004, 19: 2221−2225.
[45] XING L Q, ECKERT J, LÖSER W, SCHULTZ L. High strength materials produced by precipitation of icosahedral quasicrystals in bulk Zr−Ti−Ni−Cu−Al amorphous alloys [J]. Appl Phys Lett, 1999, 74: 664−666.
[46] MATTERN N, ECKERT J, KÜHN U. Structural behavior of $Zr_{52}Ti_5Cu_{18}Ni_{15}Al_{10}$ bulk metallic glass at high temperatures [J]. Appl Phys Lett, 2002, 80: 4525−4527.
[47] WANLUK T A, SCHROERS J, JOHNSON W L. Critical cooling rate and thermal stability of Zr−Ti−Ni−Cu−Be alloys [J]. Appl Phys Lett, 2001, 78: 1213−1215.
[48] YI S, LEE J K, KIM W T, KIM D H. Ni-based bulk amorphous in the Ni−Ti−Zr−Si system [J]. J Non-Cryst Solids, 2001, 291: 132−136.
[49] YUAN G Y, INOUE A. The effect of Ni substitution on the glass-forming ability and mechanical properties of Mg−Cu−Gd metallic glass alloys [J]. J Alloys Compd, 2005, 387: 134−138.
[50] LOUZGUINE D V, INOUE A. Investigation of structure and properties of the Al−Y−Ni−Co−Cu metallic glasses [J]. J Mater Res, 2002, 17: 1014−1018.
[51] RÉVÉSZ Á, HEUNEN G, VARGA L K, SURIÑACH S. Real time synchrotron studies on amorphous $Al_{85}Ce_5Ni_8Co_2$ and $Al_{85}Y_5Ni_8Co_2$ alloys [J]. J Alloys Compd, 2004, 368: 164−168.
[52] BASSIM N, KIMINAMI C S, KAUFMAN M J, OLIVEIRA M F. Crystallization behavior of amorphous $Al_{84}Y_9Ni_5Co_2$ alloy [J]. Mater Sci Eng A, 2001, 304−306: 332−337.
[53] FREITAG J M, KOKNAEV R G, SABET-SHARGHI R, KOKNAEVA M. Mechanical properties of Al−Y−Ni amorphous ribbons [J]. J Appl Phys, 1996, 78: 3967−3970.
[54] LOUZGUINE D V, INOUE A. Strong influence of supercooled liquid on crystallization of the $Al_{85}Ni_5Y_4Nd_4Co_2$ metallic glass [J]. Appl Phys Lett, 2001, 78: 3061−3063.
[55] CAI A H, XIONG X, LIU Y, LI J H, AN W K, LUO Y. Characteristics of near-eutectic and off-eutectic Zr−Al−Ni−Cu glass forming alloys [J]. Mater Sci Eng A, 2009, 516: 100−102.
[56] AN W K, XIONG X, LIU Y, LI J H, CAI A H, LUO Y, LI T L, LI X S. Investigation of glass forming ability and crystallization kinetics of $Zr_{63.5}Al_{10.7}Cu_{10.7}Ni_{15.1}$ bulk metallic glass [J]. J Alloys Compd, 2009, 486: 288−292.
[57] CAI A H, AN W K, LUO Y, LI T L, LI X S, XIONG X, LIU Y. Glass forming ability, non-isothermal crystallization kinetics, and mechanical property of $Zr_{61.5}Al_{10.7}Cu_{13.65}Ni_{14.15}$ metallic glass [J]. J Alloys Compd, 2010, 490: 642−646.

基于临界尺寸采用人工神经网络技术优化设计玻璃形成合金的成分

蔡安辉[1,2]，熊 翔[2]，刘 咏[2]，安伟科[1]，周果君[1]，罗 云[1]，李铁林[1]，李小松[1]，谭湘夫[1]

1. 湖南理工学院 机械工程学院，岳阳 414006；
2. 中南大学 粉末冶金国家重点实验室，长沙 410083

摘 要：建立一个用于预测和模拟玻璃形成合金的临界尺寸的人工神经网络模型；基于该人工神经网络模型优化设计一系列 Zr−Al−Ni−Cu 和 Cu−Zr−Ti−Ni 块体非晶合金的成分并对其临界尺寸进行预测。采用真空喷注法制备 Zr−Al−Ni−Cu 和 Cu−Zr−Ti−Ni 块体非晶合金试样。这些块体合金的非晶态结构采用 X 射线衍射法进行表征并确定这些合金的非晶形成的临界尺寸。结果表明，预测的临界尺寸与实验结果吻合较好，所建立的神经网络模型能可靠地设计非晶合金的成分和预测非晶合金的临界尺寸。

关键词：临界尺寸；玻璃形成合金；人工神经网络；非晶

(Edited by Hua YANG)